Can photoinhibition control phytoplankton abundance in deeply mixed water columns of the Southern Ocean?

Alderkamp, Anne-Carlijn; de Baar, Hein J. W.; Visser, Ronald J. W.; Arrigo, Kevin R.

Published in:
Limnology and Oceanography

DOI:
10.4319/lo.2010.55.3.1248

Publication date:
2010

Limnol. Oceanogr., 55(3), 2010, 1248–1264

doi:10.4319/lo.2010.55.3.1248

Can photoinhibition control phytoplankton abundance in deeply mixed water columns of the Southern Ocean?

Anne-Carlijn Alderkamp,[a,b,*] Hein J. W. de Baar,[b,c] Ronald J. W. Visser,[b] and Kevin R. Arrigo[a]

[a] Department of Environmental Earth Systems Sciences, Stanford University, Stanford, California
[b] Department of Ocean Ecosystems, Energy and Sustainability Research Institute Groningen, University of Groningen, Haren, The Netherlands
[c] Royal Netherlands Institute for Sea Research, Texel, The Netherlands

Abstract

To study how natural Southern Ocean phytoplankton communities acclimate to rapid fluctuations in irradiance levels that result from deep wind-driven mixing of the upper water column, we measured their fluorescence properties ($Fv:Fm$, maximum quantum yield of photosystem II; and qN, non-photochemical quenching) and pigment composition. Values of $Fv:Fm$ were low (< 0.46) and qN was high (> 0.67) throughout the upper mixed layer (UML). Short-term (20-min) exposure to incident surface irradiance strongly reduced $Fv:Fm$ and recovery was slow under subsequent incubation at low irradiance. This suggests that phytoplankton cells are frequently photodamaged when mixed up to the surface from depth. Recovery of $Fv:Fm$ was suppressed when lincomycin was added, inhibiting synthesis of the photosystem II reaction center D1 protein. This indicates that D1 protein repair is crucial in maintaining photosynthetic performance under fluctuating irradiance levels. Regions within the Antarctic Circumpolar Current (ACC) with a deep UML had lower depth-integrated phytoplankton biomass than regions close to the Antarctic continent with a shallow UML. Surprisingly, the depth-averaged light level within the UML in these latter regions was lower than in the ACC. Thus, it appears that photodamage incurred during the high irradiance portion of the vertical mixing cycle, rather than light limitation, controls phytoplankton growth in regions of the Southern Ocean with a deep UML. This concept represents a shift from the widely accepted paradigm that phytoplankton growth in the open Southern Ocean is limited by low levels of light or inadequate iron supply.

The Southern Ocean (south of 44°S) is an important component of the global carbon cycle due to its large size and unique physical and chemical characteristics. Recent studies indicate that some regions of the Southern Ocean are a strong sink for anthropogenic CO_2 (Arrigo et al. 2008; Gruber et al. 2009) and that its lower latitudes are important areas of anthropogenic CO_2 storage (Sabine et al. 2004). In regions south of the Polar Front, major inorganic nutrients such as nitrate, phosphate, and silicate are seldom fully utilized, but low trace metal concentrations, especially of iron (Fe), limit phytoplankton growth in large areas of the Southern Ocean (Martin et al. 1990; Boyd et al. 2007), making it the largest of the three high nutrient–low chlorophyll (HNLC) regions of the global ocean.

In addition, phytoplankton productivity is light limited in many areas of the Southern Ocean because weak water column stratification and strong winds create deep mixed layers, especially in the vicinity of the Antarctic Circumpolar Current (ACC; Mitchell et al. 1991; De Baar et al. 2005). Wind-induced vertical mixing imposes strong and rapid changes in the irradiance regime experienced by phytoplankton cells (Denman and Gargett 1983; Neale et al. 2003). This mixing reduces the total irradiance dose but periodically exposes phytoplankton to periods of excessive irradiance when residing near the surface. In response to low irradiance, algae maximize their light-harvesting capacity by increasing their photosynthetic pigment content and photosynthetic efficiency (Falkowski and La Roche 1991). In contrast, at saturating irradiance, Calvin cycle activity increases at the expense of light-harvesting pigments (Falkowski and La Roche 1991).

Irradiance exceeding photosynthetic requirements often causes photoinhibition and viability loss (Van de Poll et al. 2006). Initially, photoinhibition is associated with a decrease in functional photosystem II (PS II) reaction centers, which decreases photosynthetic activity. Progressive reduction of functional PS II limits the reducing power of antioxidant metabolism, which leads to uncontrolled formation of reactive oxygen species and eventually to loss of viability (Van de Poll et al. 2006, 2007). Photoinhibition is reversible, but recovery requires synthesis of damaged PS II components, such as the PS II reaction center D1 protein that is involved in a complex and metabolically expensive damage–repair cycle (Aro et al. 1993; Hazzard et al. 1997).

An important photoprotection mechanism is the thermal dissipation of excess energy by xanthophyll cycle pigments in their de-epoxidated state. The xanthophyll cycle of algae comprises the enzymatic conversion of carotenoids such as violaxanthin to antheraxanthin and zeaxanthin in green algae, and diadinoxanthin to diatoxanthin in diatoms (Olaizola et al. 1994; Van Leeuwe et al. 2005). Energy dissipation can be quantified in vivo by estimating non-photochemical quenching (NPQ) of chlorophyll *a* (Chl *a*) fluorescence (Demmig et al. 1987; Olaizola et al. 1994). NPQ is a result of both fast-acting energy-dependent quenching (qE), which involves the thermal dissipation of excess light-energy by xanthophyll cycle pigments, and slowly relaxing photoinhibitory quenching (qI), which has been attributed to damage or down-regulation of PS II reaction centers (Baker and Horton 1987; Oquist et al.

* Corresponding author: Alderkamp@Stanford.edu

1992) and to conformational changes in thylakoid structure (Ruban and Horton 1995). In some algal taxa, NPQ also results from state transition (qT), in which light-harvesting antennae preferentially associate with one photosystem or another (Allen 1995). The importance of qT is species specific and has never been demonstrated in diatoms.

Overall, the ability of phytoplankton to resist damage caused by excessive irradiance exposure is strongly influenced by photoacclimation and nutrient availability, both of which influence cellular pigment composition and protein turnover rates (Geider et al. 1993; Shelly et al. 2003; Van de Poll et al. 2005). There are strong interactions between Fe limitation and photoinhibition because Fe limitation decreases the synthesis of photosynthetic proteins, such as the D1 protein (Greene et al. 1992; Vassiliev et al. 1995). On the other hand, Fe-limited cells generally contain less Chl *a* but relatively more xanthophyll cycle pigments (Van Leeuwe and Stefels 1998, 2007; Van de Poll et al. 2005), which suggests that Fe-limited phytoplankton, due to their decreased capacity to absorb excess irradiance, actually may be relatively well protected against photoinhibition (Van de Poll et al. 2005; Van Leeuwe and Stefels 2007). In addition, oceanic diatoms that are adapted to grow in environments with low Fe can have fundamentally altered photosystems, with reduced amounts of Fe-rich photosystem I and cytochrome b_6f complexes (Strzepek and Harrison 2004). However, loss of cytochrome b_6f negatively affects their ability to dissipate excess energy using the xanthophyll cycle because the de-epoxidation of diadinoxanthin to diatoxanthin (necessary for the dissipation of energy) is regulated by the proton gradient across the thylakoid membrane produced through proton translocation by the cytochrome b_6f complex (Price et al. 1995; Munekage et al. 2001).

Here we report how natural phytoplankton communities acclimate to short-term variations in light conditions in the Southern Ocean. We exposed phytoplankton communities from the upper euphotic zone to incident surface irradiance and measured photoinhibition and subsequent recovery. In addition, we studied the relative importance of photoprotective vs. repair mechanisms by using an inhibitor of de novo D1 synthesis. The results of these experiments were augmented by measurements of fluorescence properties of phytoplankton in the upper water column and of their cellular proportions of photoprotective and light-harvesting pigments.

Methods

In situ sampling—This study was conducted during the first 39 d of the ANT XXIV/3 expedition on board the R/V *Polarstern* (13 February through 23 March 2008), which transited the zero meridian from Capetown, South Africa, to Antarctica, followed by a transect through the Weddell Sea (Fig. 1). Total surface downwelling irradiance was recorded continuously by the shipboard weather observatory and converted to photosynthetically available radiation (PAR). Vertical profiles of hydrographic data at 77 stations were collected using a Seabird 911+ conductivity, temperature, and depth (CTD) sensor and a Dr. Haardt fluorescence sensor. At 24 of these stations, Niskin bottles were deployed to obtain water samples from discrete depths. For these stations, we determined the relationship between Chl *a* concentration at discrete depths and fluorescence measured at those same depths obtained during vertical CTD profiling (Table 1) (*see* below). The resulting linear relationship was then used to estimate the surface Chl *a* concentration from fluorescence measurements for those stations and depths where water samples were not collected.

The attenuation of PAR in the water column was calculated using an empirical relationship between the diffuse attenuation coefficient of downwelling light K_d[PAR] and the surface Chl *a* concentration (Mathot et al. 1992):

$$K_d[\mathrm{PAR}] = 0.056 \times [\mathrm{Chl}\ a] + 0.062 \quad (1)$$

where [Chl *a*] is the mean surface Chl *a* concentration (mg m^{-3}) of the upper 20 m as derived from fluorescence. The depth of the euphotic zone, z_{EU}, defined as the depth at which the downwelling PAR falls to 1% of the value just below the sea surface, was calculated as (Kirk 1994):

$$z_{EU} = \frac{\ln(0.01)}{K_d[\mathrm{PAR}]} \quad (2)$$

The depth of the upper mixed layer (z_{UML}) was calculated from each CTD profile as the shallowest depth at which the density (σ_t) was 0.02 kg m^{-3} greater than at the surface. To calculate the total daily PAR in the upper mixed layer (E_{UML}), total daily surface PAR ($\overline{E}_{surf}$) was estimated from 8-d composites from SeaWiFS satellite PAR, and used to calculate E_{UML} (Riley 1957) in mol photons m^{-2} d^{-1}:

$$E_{UML} = \frac{\overline{E}_{surf} T (1 - e^{-K_d z_{UML}})}{K_d z_{UML}} \quad (3)$$

using mean transmittances (T) of 0.85 for the sea surface, 0.20 for gray ice and nilas, and 0.05 for snow-covered ice. Ice coverage was estimated visually and included an estimate of the aerial coverage, ice type, thickness, and snow cover characteristics (Worby et al. 1999).

Water was sampled using 12-liter Niskin bottles at 18 hydrographic stations. At 10 of these stations, short-term photoinhibition experiments were performed using phytoplankton samples from both the surface (5–10 m) and the subsurface (35–60 m) (Tables 1, 2). At 12 stations, phytoplankton samples were collected from five depths to obtain vertical profiles of fluorescence and phytoplankton pigments. All subsequent phytoplankton sample processing was carried out at ambient seawater temperature and low irradiance (< 5 μmol photons m^{-2} s^{-1}).

Chlorophyll fluorescence parameters—Maximum quantum yield of PS II ($Fv:Fm$) (Krause and Weis 1991) and the capacity for heat dissipation through non-photochemical quenching of fluorescence (Van Kooten and Snel 1990) were determined with a pulse amplified modulated (PAM) chlorophyll fluorometer (WATER-PAM chlorophyll fluo-

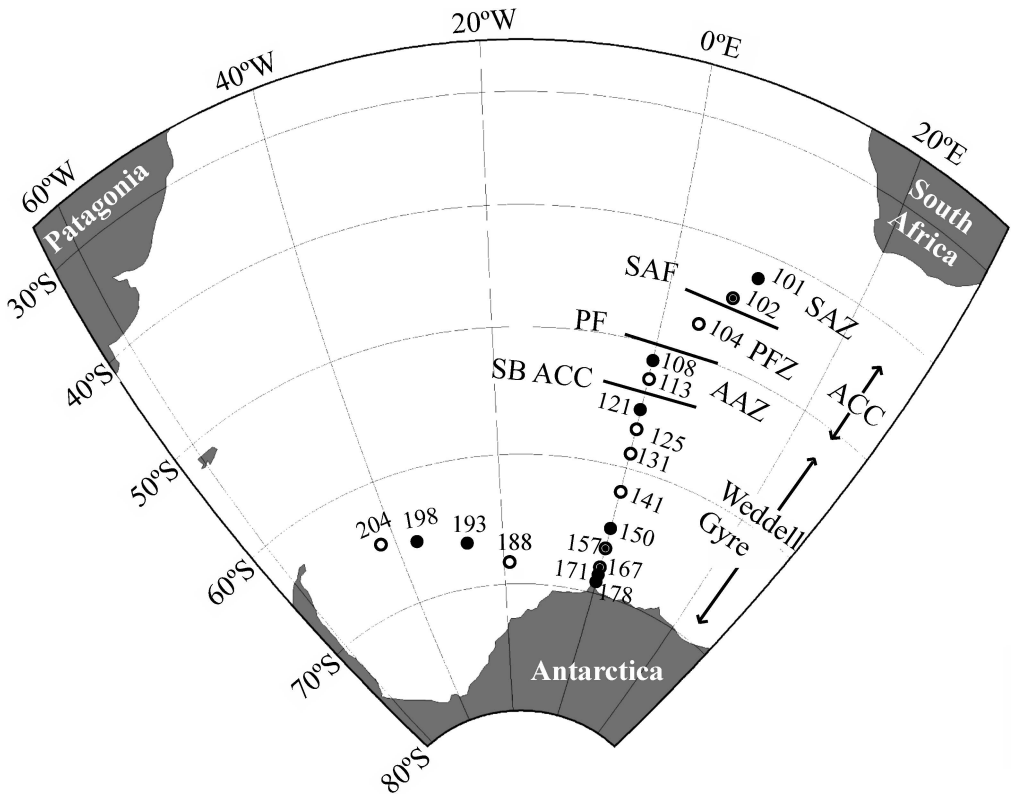

Fig. 1. Chart of the study area and stations. White dots represent 10 stations where short-term photoinhibition experiments were performed, black dots represent 12 stations where profiles of phytoplankton pigments and fluorescence properties were determined. The locations of fronts as encountered in the austral autumn 2008 are shown, and the Antarctic Circumpolar Current (ACC) and Weddell Gyre are schematically displayed. Abbreviations in alphabetical order: AAZ, Antarctic Zone; PF, Polar Front; PFZ, Polar Frontal Zone; SAF, Subantarctic Front; SAZ, Sub-Antarctic Zone; SB ACC, Southern Boundary of the ACC (locations from Middag et al. unpubl.).

rometer, Heinz Walz) and WinControl software on samples that were dark adapted for at least 30 min. This allowed for relaxation of fast quenching processes. Prolonging dark adaptation times for another 10 min did not influence the results; however, dark adaptation times longer than 1 h sometimes increased parameter values (*see* Discussion).

When the measuring light (non-photochemistry-inducing) of the PAM was turned on, the minimum fluorescence (*Fo*) of the sample was measured. The maximum fluorescence (*Fm*) was then measured by applying a saturating light pulse of 4000 μmol photons m^{-2} s^{-1} for 0.8 ms, in order to close all PS II reaction centers. The *Fv*:*Fm* was calculated as

$$Fv : Fm = \frac{Fm - Fo}{Fm} \quad (4)$$

After a 12-s delay, the actinic (photochemistry-inducing) light source of 670 μmol photons m^{-2} s^{-1} was turned on for 200 s, allowing the fluorescence signal to reach a steady-state balance between fluorescence, photochemistry, and non-photochemical energy pathways (defined as *Fs*). The actinic light period was followed by another saturating light pulse to determine *Fm′*, defined as the maximum PS II fluorescence in light-acclimated cells. Directly after this second saturating light pulse following the actinic light period, the minimum fluorescence in the light (*Fo′*) was measured. Taking variable *Fo* baselines during each analysis into account, non-photochemical quenching (*qN*) was calculated as

$$qN = 1 - \frac{Fm' - Fo'}{Fm - Fo} \quad (5)$$

At each station, blanks were run on GF/F filtrates. By using unconcentrated samples from regions with low phytoplankton biomass for our analysis, the fluorescence levels were close to the detection limit of the PAM fluorometer. This resulted in significant variations in the fluorescence *Fo* baseline under the measuring light. To ensure reproducibility, measurements of *Fv*:*Fm* were repeated at least three times and *qN* was measured twice. Data were not included if replicates differed by more than 0.05 for *Fv*:*Fm* and 0.1 for *qN* (which was observed for some *qN* measurements of low-biomass samples from 100-m depth). Data from three profiles obtained in areas of low phytoplankton biomass were omitted because replicates showed excessive variation in both *Fv*:*Fm* and *qN*.

An alternative way of determining non-photochemical quenching is to measure the ratio of change in *Fm* to the final value of *Fm* (Bilger and Björkman 1990; Maxwell and Johnson 2000). However, because of variations in the

Table 1. Overview of supporting data of the 18 stations sampled for this study on the ANT XXIV/3 expedition aboard R/V *Polarstern*. Fourteen stations (101–178) were sampled following a transect along the zero meridian, and four stations (188–204) were sampled following a transect through the Weddell Sea. Water temperature and nutrient data are the average of the surface 50 m (full set of nutrient data R. Middag unpubl.; full set of dissolved Fe [dFe] data M. Klunder unpubl.).*

Sta.	P or E	Date	Position (lat)	Position (long)	z_{UML} (m)	Daily PAR (mol photons m^{-2} d^{-1})	PAR at time of sampling (μmol photons m^{-2} s^{-1})	NO_x (μmol L^{-1})	PO_4 (μmol L^{-1})	Si (μmol L^{-1})	dFe (nmol L^{-1})	Water temp. (°C)	Sampling time (hh:mm after sunrise)
101	P	13 Feb 08	42°20′S	8°60′E	30	37.1	797	12.70	0.89	0.73	0.26	11.2	08:55
102	P, E	15 Feb 08	44°40′S	7°50′E	68	25.5	814	16.46	1.17	0.66	n.a.	9.1	04:00
104	E	17 Feb 08	47°38′S	4°16′E	86	24.9	808	19.73	1.37	2.81	n.a.	6.5	07:55
108	P	19 Feb 08	51°30′S	0°0′E	96	11.9	334	23.00	1.50	11.33	n.a.	3.0	01:40
113	P, E	20 Feb 08	53°00′S	0°0′E	109	25.4	859	26.05	1.73	35.31	0.2	1.3	04:40
121	P	22 Feb 08	55°30′S	0°0′E	50	24.6	23	25.41	1.74	52.94	n.a.	0.7	00:00
125	E (control)	23 Feb 08	57°00′S	0°0′E	112	11.9	2	n.a.	n.a.	n.a.	n.a.	0.5	00:00
131	E	25 Feb 08	59°00′S	0°0′E	70	12.9	338	26.39	1.84	64.97	0.16	0.2	03:30
141	E	27 Feb 08	62°0′S	0°0′E	51	16.3	435	24.08	1.76	56.50	0.25	0.4	03:30
150	P	29 Feb 08	65°0′S	0°0′E	32	17.0	257	25.29	1.67	64.31	0.26	−0.5	01:45
157	P, E	07 Mar 08	66°31′S	0°3′W	29	22.7	105	26.82	1.77	62.99	n.a.	−0.7	08:25
167	P, E	10 Mar 08	68°00′S	0°3′W	42	14.9	221	26.02	1.72	63.67	0.10	−0.7	01:05
171	P	10 Mar 08	68°45′S	0°0′E	44	14.9	114	25.89	1.71	59.28	n.a.	−0.9	12:00
178	P	12 Mar 08	69°24′S	0°0′E	28	3.4	2	24.82	1.77	53.98	0.32	−1.6	00:00
188	E	16 Mar 08	68°24′S	19°3′W	41	21.2	157	27.70	1.96	68.23	n.a.	−1.8	01:00
193	P	19 Mar 08	66°35′S	27°23′W	50	7.2	270	28.06	1.91	73.62	0.11	−1.8	04:10
198	P	21 Mar 08	65°38′S	36°22′W	65	4.2	135	28.01	1.88	73.63	0.05	−1.4	01:45
204	E	23 Mar 08	64°48′S	42°51′W	35	6.9	527	26.56	1.80	69.98	0.06	−1.8	02:40

* P, profile of the top 100 m; E, surface irradiance exposure experiment; PAR, photosynthetically available radiation; temp., temperature; n.a., not available.

Table 2. Supporting data for the surface irradiance exposure experiments. The sampling depth of the surface (S) and subsurface (D) samples, and the PAR_{exp} is the average photosynthetically available radiation level during 20 min of surface irradiance exposure. (dd + dt) : Chl a_{d+h} is the protective pigment ratio, i.e., the pool of both epoxidated (diadinoxanthin [dd]) and de-epoxidated (diatoxanthin [dt]) xanthophyll cycle pigments normalized to the Chl *a* concentration from diatoms and haptophytes as derived from the CHEMTAX analysis. Dominant phytoplankton group (% of total Chl *a*) as derived from CHEMTAX analysis.

Sta.	Sample depth (m) (S) (D)	PAR_{exp} (μmol photons m^{-2} s^{-1})	(dd+dt) : Chl a_{d+h}	Dominant phytoplankton group	2nd dominant phytoplankton group
102	10	848	0.21	Chlorophytes (55%)	Haptophytes (32%)
	50		0.22		
104	10	368	0.32	Chlorophytes (45%)	Haptophytes (33%)
	60		0.20		
113	5	986	0.23	Diatoms (61%)	Haptophytes (23%)
	50		0.12		
125 (control)	5	58	0.21	Diatoms (58%)	Chlorophytes (21%)
	50		0.21		
131	5	449	0.32	Diatoms (41%)	Chlorophytes (36%)
	50		0.12		
141	5	611	0.19	Haptophytes (60%)	Chlorophytes (29%)
	50		0.13		
157	5	415	0.18	Diatoms (68%)	Haptophytes (21%)
	45		0.05		
167	5	97	0.18	Diatoms (80%)	Chlorophytes (12%)
	40		0.16		
188	5	565	0.11	Diatoms (68%)	Haptophytes (23%)
	50		0.13		
204	5	559	0.16	Diatoms (74%)	Chlorophytes (13%)
	35		0.16		

baseline *Fo* between the time of measuring *Fm* and *Fm′*, this did not lead to reproducible values of NPQ.

Pigments—We filtered 1.0–2.5 liters of seawater through a GF/F filter, which was immediately flash frozen in liquid nitrogen and stored at −80°C until analysis. The filters were freeze-dried (48 h) and extracted in 90% acetone (48 h), and pigments were separated on a high-performance liquid chromatography (HPLC) system (Waters 2690 separation module, 996 photodiode array detector) using a C_{18} 5-μm DeltaPak reverse-phase column (Kraay et al. 1992; Van Leeuwe et al. 2006). Quantification was done using standard dilutions of Chl *a*, *b*, c_3, 19′-butanoyloxyfucoxanthin (but), fucoxanthin (fuc), 19′-hexanoyloxyfucoxanthin (hex), diadinoxanthin (dd), diatoxanthin (dt), violaxanthin (violax), alloxanthin (allox), zeaxanthin (zeax), and peridinin (per). In addition, beta-carotene and the Chl *a* breakdown (or intermediate) product chlorophyllide *a* were analyzed but detected in very small amounts and, therefore, are not presented.

The CHEMTAX matrix factorization program, version 1.95 (Mackey et al. 1996; Wright et al. 1996) was used to assess phytoplankton class abundances. The program uses the steepest descent algorithm to determine the best fit based on an estimate of pigment : Chl *a* ratio for different algal classes. The initial database included a Southern Ocean data set containing prasinophytes, cryptophytes, two types of diatoms (one with a pigment ratio specific for *Pseudonitzschia* and one for Antarctic diatoms without Chl c_3), chlorophytes, and two types of haptophytes (type 6 with a pigment ratio specific for *Emiliania huxleyi* and type 8 specific for *Phaeocystis antarctica*) (Zapata et al. 2004; Wright et al. 2009). The presence of these groups was confirmed by microscopic analysis (M. Roberts and K. Bluhm pers. comm.). Dinoflagellates were omitted because the marker pigment peridin was detected only in a few samples and in very small amounts, and microscopic analysis confirmed that dinoflagellates were never abundant. Type 6 haptophytes contributed considerably to the phytoplankton biomass south of the Polar Front, where *E. huxleyi* is unlikely to occur. The difference between type 6 and type 8 haptophytes is based on different ratios of but, fuc, and hex; however, these ratios are highly variable in different strains of *P. antarctica* (Zapata et al. 2004) and are affected by nutrient status, notably Fe limitation (Van Leeuwe and Stefels 1998). The final ratios of these pigments derived from the steepest descent algorithm for type 6 haptophytes were within the range of those reported for *P. antarctica* (Zapata et al. 2004) and, thus, the two types of haptophytes produced by CHEMTAX were pooled such that north of the Polar Front, they comprise both *E. huxleyi* and *Phaeocystis* sp., whereas south of the Polar Front, they are assumed to represent solely *P. antarctica*.

The potential photoprotective role of xanthophyll cycle pigments for diatoms and haptophytes was evaluated by measuring the pool of both epoxidated (diadinoxanthin [dd]) and de-epoxidated (diatoxanthin [dt]) xanthophyll cycle pigments normalized to the Chl *a* concentrations of these two phytoplankton groups (dd + dt : Chl a_{d+h}). In diatoms and haptophytes, non-photochemical quenching is specifically related to the presence of dt (Olaizola et al. 1994). However, because xanthophyll cycle pigments are

epoxidated on a timescale of minutes (Van de Poll et al. 2006), shorter than the time required to process and filter samples, only trace amounts of dt were detected in some samples. Therefore, we used the sum of dd + dt (normalized to Chl a_{d+h}) to characterize the potential for xanthophyll cycle photoprotection (Van de Poll et al. 2005, 2006). Xanthophyll cycling in chlorophytes (VAZ cycle) could not be evaluated because only trace amounts of violaxanthin and zeaxanthin were detected in stations north of the Polar Front where chlorophytes were most abundant.

Short-term surface irradiance exposure experiments—The sensitivity of phytoplankton growing in the upper water column to surface irradiance levels (Table 1) and subsequent recovery under low irradiance was assessed in short-term surface irradiance experiments (Table 2). At 10 stations (Table 1), experiments were carried out with phytoplankton sampled from two depths: the surface (S, 5–10 m) and the Chl *a* maximum (D, 35–60 m). When no deep Chl *a* maximum was detected, subsurface water was obtained from a depth of 50 m (Table 2). Two treatments were tested, one with no addition of inhibitor and the other with the addition of 0.6 mmol L^{-1} (final concentration) lincomycin (Sigma, from a 100× stock solution freshly prepared in 96% ethanol). Lincomycin inhibits transcription of chloroplast-encoded proteins such as the D1 reaction center protein (Bouchard et al. 2005*a*). Experiments were carried out in triplicate, and a single control sample for each treatment was not exposed to surface irradiance but kept at low light (2 μmol photons m^{-2} s^{-1}) and ambient seawater temperature.

Samples were filtered for HPLC analysis and the fluorescence properties ($Fv:Fm$ and qN) of each sample were determined by PAM-fluorometry as described above. Samples were incubated for 20 min at incident irradiance and in situ seawater temperature, floating at the surface of a deck incubator in 50-mL polystyrene culture flasks (Becton Dickinson). The polystyrene flasks were transparent to both PAR and ultraviolet (UV)A, whereas UVB was blocked, which was confirmed by measuring absorption of the flask between 200 and 800 nm on a Perkin-Elmer Lambda 35 spectrophotometer. After 20 min of exposure to surface irradiance, subsamples were removed and $Fv:Fm$ was determined after dark acclimation for 5 min. Samples were then kept at low light (2 μmol photons m^{-2} s^{-1}) under cool white fluorescent lamps at ambient seawater temperature to monitor recovery. The capacity of D1 protein synthesis needed for repair of photodamage in vivo is saturated at very low irradiance or photon exposure (Anderson et al. 1997; Bouchard et al. 2006). Recovery of $Fv:Fm$ was followed for 2 h at time intervals of ~ 30 min after 5 min of dark acclimation. A dark acclimation period of only 5 min allowed us to resolve the fast-relaxing quenching, so that both fast- and slow-relaxing quenching influenced the reduction in $Fv:Fm$ after surface irradiance exposure. Tests showed that the length of dark acclimation (2, 5, 10 min) did not affect $Fv:Fm$ values measured later than time point (T) 50 min after the start of the experiment (30 min after surface irradiance exposure), indicating that fast-relaxing quenching had relaxed after this time during the recovery period when phytoplankton were incubated at low light intensity.

To test if handling of the samples during the experiment influenced fluorescence characteristics, a control experiment was performed at sunrise on 23 February under low (58 mol photons m^{-2} d^{-1}) surface irradiance. In this experiment the $Fv:Fm$ of all samples was slightly reduced after exposure to these low surface irradiance conditions but rebounded to initial values rapidly during recovery under low light, showing that handling of the samples did not result in photoinhibitory quenching.

Standard trace metal clean procedures were not followed during the incubations, but contamination with trace metals is unlikely to have an effect given the short time frame of the incubations. $Fv:Fm$ is the first parameter to respond to additions of trace metals in HNLC regions and it takes several hours to days to observe a response (Behrenfeld et al. 1996; Boyd et al. 2000). Consistent with our assumption that trace metal contamination did not affect our results, $Fv:Fm$ did not increase in any of the experimental controls in D samples, although the $Fv:Fm$ did increase in three out of eight experimental controls of the S samples. We attribute this increase to slow-relaxing quenching related to repair of photodamage, similar to what was observed during the recovery period after surface irradiance exposure.

The fast-relaxing energy-dependent quenching (qN_F) and slow-relaxing photoinhibitory quenching (qN_S) components of qN for phytoplankton samples were analyzed in experimental treatments without addition of an inhibitor following the approach presented in Maxwell and Johnson (2000), using the qN instead of NPQ. Measurements of qN from time points after 30 min of recovery (T = 50 min) were linearly regressed against time and extrapolated back to the time immediately after surface irradiance exposure (T = 20 min) to determine the value of qN that would have been attained if only slowly relaxing quenching had been present during recovery under low light conditions (qN_S). Rapidly relaxing quenching (qN_F) was then calculated as the difference between qN_S and qN_I, the qN measured immediately after exposure to surface irradiance.

Statistics—Data were checked for normality using the Kolmogorov–Smirnov test. The initial response of the phytoplankton $Fv:Fm$ after surface irradiance exposure was tested with one-way ANOVA, followed by post hoc Tukey's tests. The recovery response was tested with a repeated-measures ANOVA, using Statistica software (release 7, StatSoft). Relationships between surface parameters were tested using simple linear regression analysis.

Results

Hydrographic setting, Chl a *distribution, and phytoplankton community composition*—Surface water concentrations of silicate, nitrate, and phosphate were high (> 40, > 20, and > 1.5 μmol L^{-1}, respectively) throughout the entire study area south of the Polar Front (Table 1). In contrast, silicate concentrations were as low as 0.5 μmol L^{-1} in the Sub-Antarctic Zone (SAZ), whereas nitrate and phosphate

concentrations were still elevated (> 10 and 1.0 μmol L^{-1}, respectively). Along the zero meridian (Fig. 1), concentrations of dissolved Fe (dFe) were between 0.12 and 0.35 nmol L^{-1}), with the lowest values observed near the edge of the continental ice sheet between 67°S and 69°S. Concentrations of dFe in the Weddell Sea were lower still, with values approximating 0.05 nmol L^{-1} throughout the transect (M. Klunder unpubl.).

Along the zero meridian transect, mixed layers were deep (> 100 m) within the Polar Frontal Zone and the Antarctic Zone of the Antarctic Circumpolar Current (ACC), with z_{UML} generally exceeding z_{EU} (Fig. 2A) and coinciding with low phytoplankton biomass (Fig. 2G). At stations within the ACC where z_{UML} was reduced (50–60 m), there was a pronounced relic mixed layer located deeper in the water column. South of the ACC (60°S), z_{UML} was generally ~ 40 m and shallower than the z_{EU} (Fig. 2A). Here, phytoplankton biomass was higher (Fig. 2G), reaching Chl *a* concentrations of 0.8 mg m^{-3}. The low values of dFe (M. Klunder unpubl.) and dissolved manganese (R. Middag unpubl.) in surface waters indicate drawdown of micronutrients by phytoplankton. On the shelf south of 69.5°S, the upper mixed layer (UML) deepened and Chl *a* was enhanced throughout the upper 70 m of the water column.

Phytoplankton community structure (Fig. 2E) followed the trends in macronutrients, with chlorophytes and haptophytes dominating the SAZ stations north of the Polar Front where silicate was depleted. Diatoms dominated all stations south of the Polar Front, with the exception of Sta. 141, which was dominated by the haptophyte *P. antarctica*. Prasinophytes were observed north of the Polar Front within the Chl *a* maximum at 50-m depth and in the Western Weddell Sea in samples deeper than 50 m. There were minor differences in phytoplankton community composition with depth, with haptophytes slightly more abundant at deeper stations (results not shown).

Levels of incident surface PAR and total daily PAR in the upper mixed layer (E_{UML}) were highest at stations within the SAZ, with E_{UML} of ~ 10 mol photons d^{-1} and maximum incident PAR during the day exceeding 1500 μmol photons m^{-2} s^{-1} (Table 1). Incident PAR decreased rapidly further south due to decreasing day length and solar elevation angle. This, in combination with a deepening z_{UML}, strongly decreased E_{UML} within the ACC and the Weddell Gyre (Fig. 2C). Over the zero meridian transect, depth-integrated (100-m) Chl *a* (mg m^{-2}) was negatively correlated with z_{UML} (Table 3), indicating that a deep z_{UML} was limiting phytoplankton growth. Surprisingly, there was a negative correlation between depth-integrated Chl *a* and E_{UML} (Table 3), indicating that phytoplankton biomass was greater in areas with a lower E_{UML}.

In the Weddell Sea, both z_{UML} (Fig. 2B) and E_{UML} (Fig. 2D) were similar to values along the zero meridian section in the Weddell Gyre. Phytoplankton biomass in the water column reached levels of 0.6 mg Chl *a* m^{-3} in the central Weddell Sea. Ice cover in the eastern and western part of the Weddell Sea (Fig. 2D) limited light penetration in the water column and, in these areas, phytoplankton biomass was low (Fig. 2H). The phytoplankton community was dominated by diatoms, similar to the southern stations of the zero meridian transect (Fig. 2F).

No significant correlation between the depth-integrated Chl *a* and z_{UML} was observed in the Weddell Sea (Table 3), although depth-integrated Chl *a* was positively correlated with E_{UML}, indicating that low light levels were limiting phytoplankton growth, especially in areas with ice cover.

Profiles of phytoplankton pigment and fluorescence properties—Pigment ratios showed clear changes over depth in almost all profiles (Fig. 3), with the Chl c_3 : Chl *a* ratio increasing with depth while the (dd + dt) : Chl *a* and fuc : Chl *a* ratios decreased. Although there were generally only weak pigment gradients within the UML, there were clear differences in pigment ratios between the UML and greater depths. These pigment ratio profiles suggest that phytoplankton optimized their pigment composition to acclimate to changes in the light climate, even when they were mixed below the mixed layer. Furthermore, the absence of strong gradients within UML suggests that mixing rates are higher than rates of photoacclimation, similar to observations made under controlled fluctuating light regimes (Van de Poll et al. 2007; Kropuenske et al. 2009). Below the UML, depth-dependent trends in pigment ratios varied by station without a consistent pattern.

The *Fv* : *Fm* in surface samples was low at all stations on the zero meridian transect as well as in the Weddell Sea (Fig. 4). The highest surface *Fv* : *Fm* (0.47) was detected on the southernmost station of the meridian transect, whereas the surface *Fv* : *Fm* was < 0.40 at all other stations. Most profile stations showed an increase in *Fv* : *Fm* with depth. Because there was no corresponding trend in dFe concentrations in the top 100 m (M. Klunder unpubl.), the low surface *Fv* : *Fm* values were likely due to photoinhibition by high irradiance levels at the surface. In some stations, there was a gradual increase of *Fv* : *Fm* with depth within the UML (e.g., Sta. 102, 113, 193), although in most stations, the main increase was below the z_{UML} (e.g., Sta. 101, 150, 157).

The non-photochemical quenching parameter (*qN*) at the surface was high at all stations (0.67–1.0, with 1.0 being the maximum possible *qN*). In some stations, there was a gradual decrease in *qN* within the UML (e.g., Sta. 101, 102, 193), whereas at most stations, *qN* remained high throughout the UML (e.g., Sta. 150, 157, 167, 171). Most of the profile stations showed a decrease in *qN* below the UML.

Short-term surface irradiance exposure experiments—Exposure to surface irradiance (Table 2) for 20 min caused a strong reduction in *Fv* : *Fm* in all experimental treatments (Fig. 5), relative to the controls that were not exposed. In general, the depth from which the samples were collected did not affect the initial *Fv* : *Fm* response (ANOVA, $p > 0.05$), except for samples from Sta. 188 ($p = 0.047$), where the reduction in *Fv* : *Fm* was stronger in S than in D samples. Also, the addition of lincomycin did not affect the

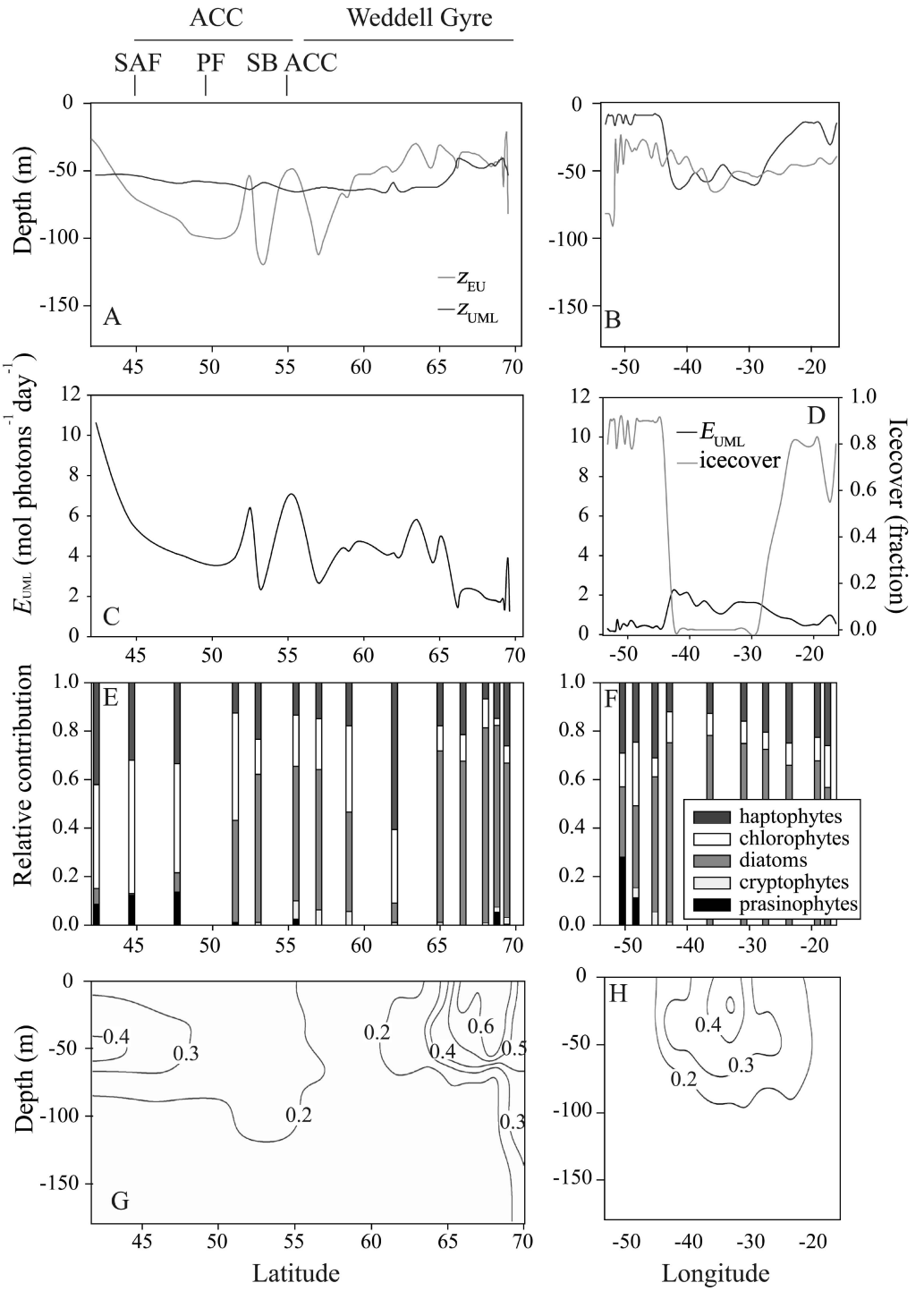

Fig. 2. (A, C, E, G) Section graphs of the meridian transect and (B, D, F, H) the transect through the Weddell Sea. The locations of the fronts are indicated above the figure, abbreviations as in Fig 1. (A, B) The depth of the upper mixed layer (z_{UML}) and the euphotic zone (z_{EU}) on the (A) zero meridian and (B) Weddell Sea transect. (C, D) The mean daily irradiance available to phytoplankton in the UML on (C) the zero meridian where no ice cover was observed and (D) the Weddell Sea where fraction of ice cover is also plotted. (E, F) The phytoplankton class contribution averaged over the surface 50 m as resolved from pigment composition by the CHEMTAX program. (G, H) Fluorescence sections of (G) the zero meridian and (H) Weddell Sea. Fluorescence values are scaled to approximate Chl *a* concentrations based on pigment concentrations collected on discrete depths of 24 stations and analyzed by HPLC.

Table 3. Correlations in simple linear regressions of the phytoplankton level of factor 1, the Chl *a* integrated over the surface 100 m of the ocean (ΣChl *a* mg m^{-2}) and factor 2, either the depth of the upper mixed layer (z_{UML} in m) or the mean irradiance available to the phytoplankton in the upper mixed layer (E_{UML} in mol photons m^{-2} d^{-1}) for stations in the meridian section and the Weddell section.

Sector	Factor 1	Factor 2	Equation	*n*	R^2	*p*
Meridian	ΣChl *a*	z_{UML}	Chl $a=-0.82\times[z_{UML}]+83.35$	37	0.186	<0.01
Meridian	ΣChl *a*	E_{UML}	Chl $a=-0.08\times[E_{UML}]+6.07$	37	0.316	<0.001
Weddell	ΣChl *a*	z_{UML}	Chl $a=0.21\times[z_{UML}]+43.79$	36	0.015	0.48
Weddell	ΣChl *a*	E_{UML}	Chl $a=0.03\times[E_{UML}]+0.13$	36	0.302	<0.001

initial response to surface irradiance exposure (ANOVA, $p > 0.05$), except for samples from Sta. 104 ($p = 0.012$).

The phytoplankton *Fv*:*Fm* recovered when they were shifted to low irradiance in all experiments (Fig. 5), except for samples from Sta. 204, for which no recovery was observed. In all other experiments, recovery was negatively affected by the inhibition of D1 repair through the addition of lincomycin (repeated-measures ANOVA, $p < 0.05$). In four of the experiments, the addition of lincomycin almost completely blocked recovery. The effect of lincomycin was smallest in the samples from Sta. 167, which was conducted at relatively low PAR (97 μmol photons m^{-2} s^{-1}). These results indicate that D1 protein repair is an important response mechanism for phytoplankton exposed to surface levels of irradiance at all stations that were tested.

Although there were small differences between the recovery of phytoplankton in S and D samples, these differences were not significant (repeated-measures ANOVA, $p > 0.05$), except for the samples from Sta. 157 ($p = 0.012$), where S samples recovered faster than D samples (Fig. 5). Sta. 157 was the only station where the D sample was taken from below the UML.

The potential photoprotective xanthophyll cycle pigment ratio for diatoms and haptophytes (dd + dt : Chl a_{d+h}) varied between 0.11 and 0.32 in the surface samples (Table 2). Corresponding to the phytoplankton response to the surface irradiance exposure, there was little difference in xanthophyll cycle pigments between the S and D samples in most stations, although occasionally the ratio in the D sample was lower. This was most notable in Sta. 157, where the D sample was taken from below z_{UML}, whereas in other stations, both the S and the D samples were taken from the UML.

The quenching measured directly after exposure to surface irradiance (qN_I) was close to its maximum value of 1 in almost all experiments (Fig. 6). Analyses of qN_S and qN_F confirmed that qN_S, the component that is related to photoinhibitory quenching, was the major component of qN_I after exposure to surface irradiance conditions in virtually all experiments. The lone exception was for Sta. 167, which had the lowest levels of PAR during the entire experiment (Table 2). When both the S and the D samples were taken into account, qN_S was positively correlated with PAR during exposure (Table 4) while qN_F was negatively correlated with PAR. In the experiments performed on the zero meridian transect, there was a weak, negative correlation between qN_F and z_{UML} (Table 4). This suggests that growth in deep UMLs reduces the capacity of phytoplankton for photoprotective non-photochemical quenching. Finally, there were no significant relationships between both qN_S and qN_F and either the (dd + dt) : Chl a_{d+h} or E_{UML}.

Discussion

It has been suggested that primary productivity by phytoplankton in regions of the Southern Ocean with deep wind-driven vertical mixing is hampered by a combination of light limitation and iron limitation (De Baar et al. 2005). Correspondingly, we encountered low phytoplankton biomass in waters of the ACC that had a deep z_{UML} and higher phytoplankton biomass in waters close to the Antarctic continent having a much shallower z_{UML}. However, despite its deeper mixed layer, total daily PAR in the upper mixed layer (E_{UML}) was actually higher in the ACC region than in waters near the Antarctic continent. In addition, surface concentrations of dFe were relatively high near the Polar Front, approximately twice that of waters south of 60°S where phytoplankton biomass was high and drawdown of dFe was substantial (M. Klunder unpubl.). These results indicate that neither light nor Fe availability was the major limiting factor of phytoplankton growth in the ACC.

Furthermore, in the short-term surface irradiance exposure experiments, we observed strong photoinhibition and photodamage in phytoplankton cells exposed for only 20 min to surface irradiance at all stations tested. Even under relatively low surface irradiance, phytoplankton cells had to repair damage to their photosystems, and suffered a loss of PS II efficiency for up to an hour. Therefore, we propose that the photodamage incurred during the high-light portion of the mixing cycle in regions with a deep z_{UML} prevents phytoplankton from photosynthesizing maximally under fluctuating light conditions. This is supported by the high degree of non-photochemical quenching and photoinhibition observed in the in situ fluorescence profiles. The agreement between high values of qN throughout the UML in the profiles and the high values of qN_S in the experiments suggests that the experiments are good representations of conditions in the UML. The phytoplankton experience photodamage when mixed up to the surface and need considerable time for repair of photodamage when mixed down. In this way, photoinhibition reduces productivity, even at depth where light levels are too low for photoinhibition. To our knowledge, this is the first study showing that photoinhibition associated with fluctuating light, rather than light limitation, is an important control on phytoplankton growth in regions of the Southern Ocean with a deep z_{UML}.

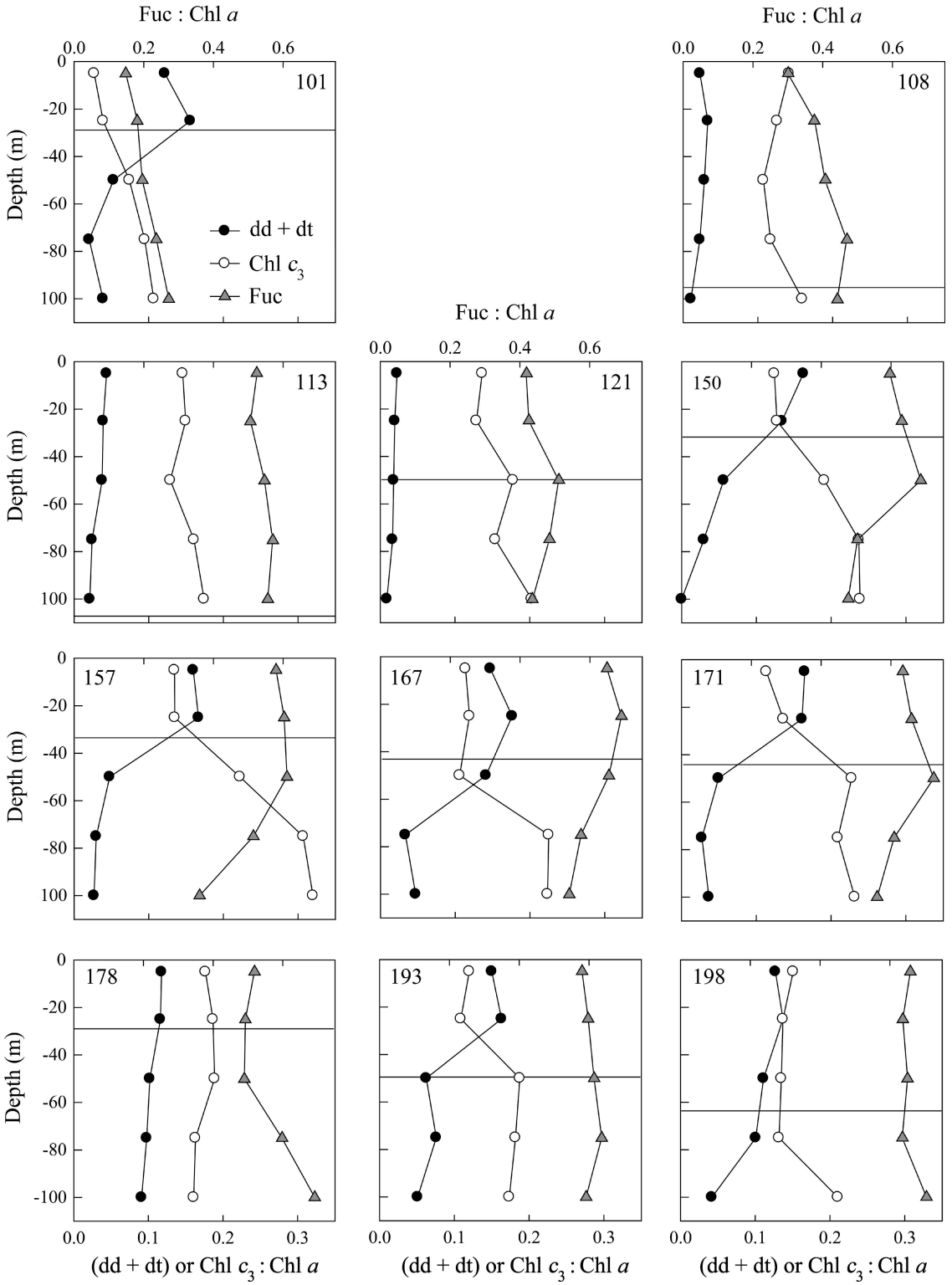

Fig. 3. Vertical profiles of phytoplankton pigment ratios expressed per Chl *a*. The depth of the upper mixed layer (z_{UML}) is indicated by a black line. Station numbers are shown on the upper corners of each panel.

In this study we used fluorescence to estimate Chl *a* concentrations, which were used as a proxy for phytoplankton biomass. Fluorescence generally gives realistic estimates of the Chl *a* concentrations, but high irradiance may decrease the fluorescence yield of phytoplankton Chl *a* in surface waters (Holm-Hansen et al. 2000). However, since the stations were sampled at different times during the day and night with variable in situ irradiance levels, the

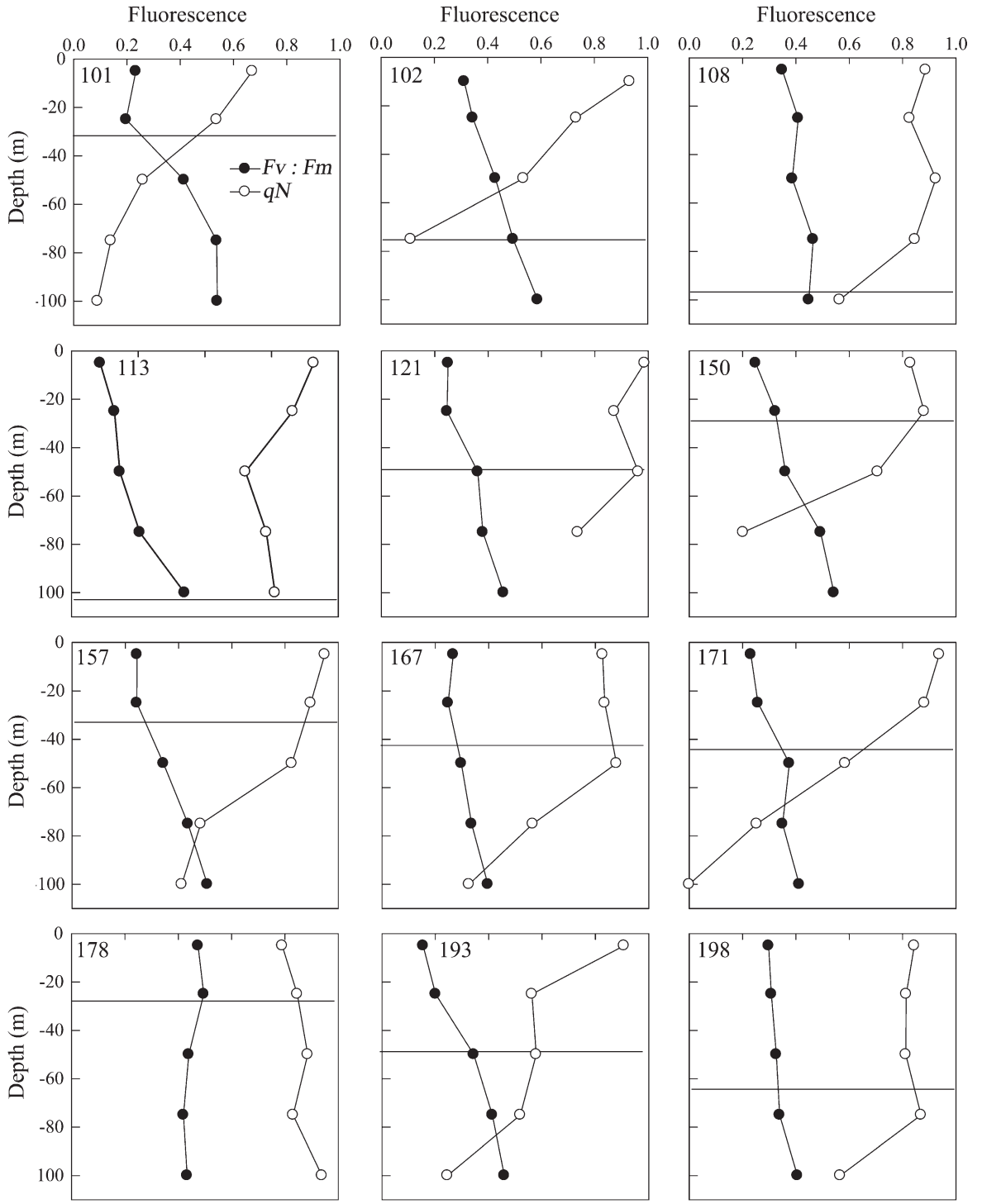

Fig. 4. Vertical profiles of phytoplankton fluorescence properties. The depth of the upper mixed layer (z_{UML}) is indicated by a black line. Station numbers are shown on the upper corners of each panel.

effect of light on Chl *a* fluorescence yield varied by station and not by region in our study. Therefore, variable fluorescence yield likely did not affect the relationships between phytoplankton biomass and E_{UML} or z_{UML}. In addition, cellular phytoplankton Chl *a* concentrations decrease under Fe limitation (Greene et al. 1992; Geider et al. 1993) and increase under light limitation (Falkowski and La Roche 1991; Van de Poll et al. 2007). Both the dFe concentrations and the ambient light levels are higher in the ACC region than at stations on the zero meridian transect close to the edge of the Antarctic continental ice sheet. Therefore, we expect that the effects of higher light and low

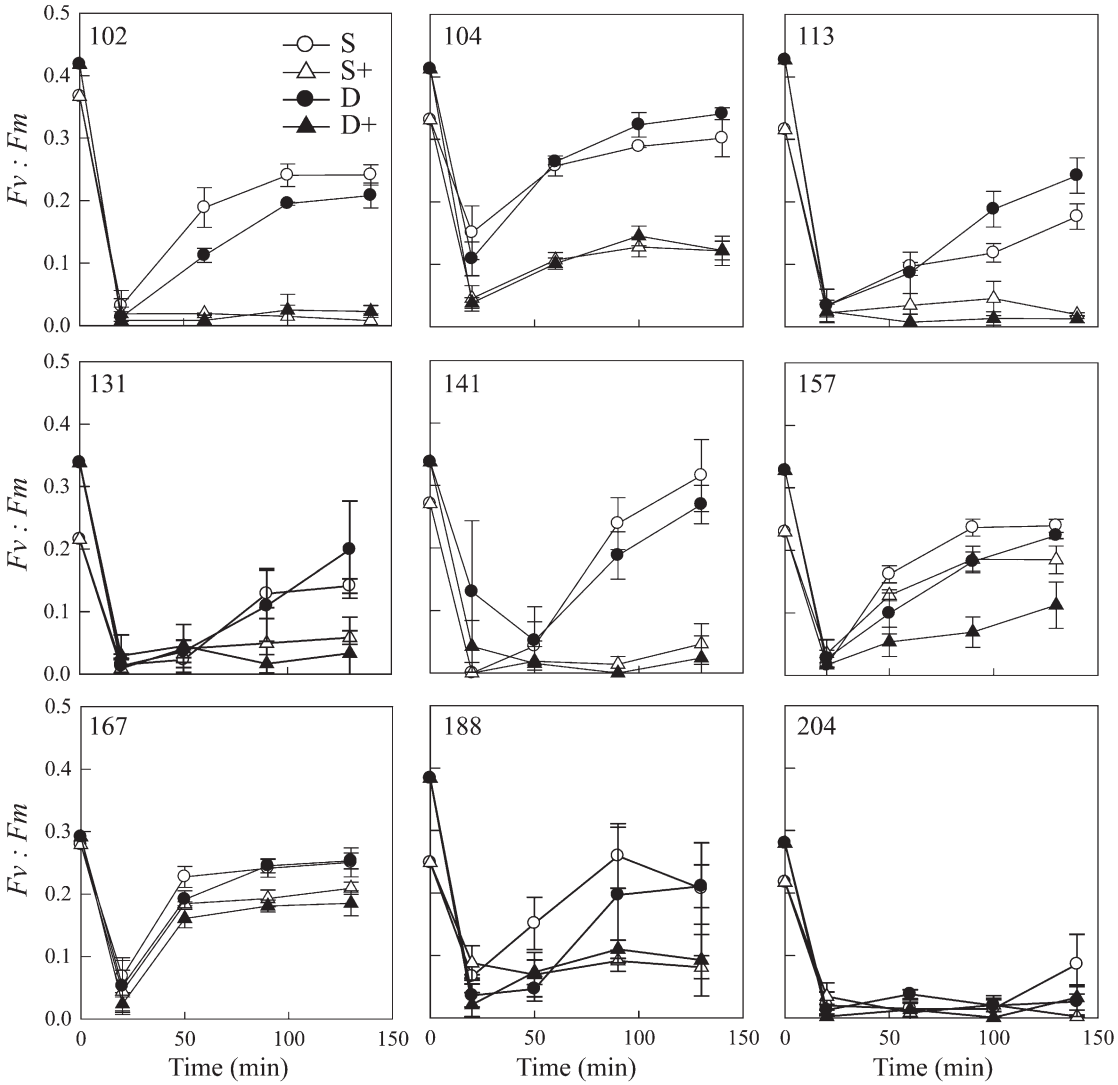

Fig. 5. Results of the short-term photoinhibition experiments. PS II efficiency ($Fv:Fm$) dynamics after exposure to surface irradiance conditions for 20 min and subsequent recovery at low irradiance. Mean and standard deviation are shown for three replicates from the surface (S, 5–10-m depth), and the subsurface (D, 40–60-m depth), of untreated phytoplankton samples and samples with the addition of lincomycin (+), an inhibitor of repair of the D1 core protein of PS II. Station numbers are shown on the upper corners of each panel.

Fe on the phytoplankton cellular Chl *a* to offset each other, and thus only mildly affect the net cellular Chl *a* concentrations over the meridian transect.

Timescales of photoacclimation—Phytoplankton growth in the UML requires that cells adjust their photosynthetic machinery in response to changes in their light environment. As the mean incident irradiance decreases, cells increase their cellular photosynthetic pigment concentrations and decrease their cellular photoprotective pigment content. This was apparent in the changes in pigment ratios we observed in cells collected from below the z_{UML} (Fig. 3). The opposing depth-dependent trends in the Chl c_3 : Chl *a* (Chl c_3 is an accessory photosynthetic pigment) and (dd + dt) : Chl *a* ratios (xanthophyll cycle pigments are photoprotective) with depth show that changes in cellular Chl *a* in response to changes in light levels (Falkowski and La Roche 1991) cannot be the sole explanation for the differences in pigment ratios over depth. Rather, cells acclimate by changing their full suite of pigments, both photosynthetic and photoprotective (Van Leeuwe and Stefels 1998; Van de Poll et al. 2006).

Acclimation to changes in light level takes place at multiple timescales. Short-term photoprotection mechanisms, such as xanthophyll cycling and the resulting fast-relaxing non-photochemical quenching, are vital to phytoplankton in withstanding short periods (minutes–hours) of high light exposure (Kulheim et al. 2002; Lavaud et al. 2002). On longer timescales (days–weeks), however, cells in fluctuating light environments need to balance their photosynthetic machinery to maximize photoprotection at high light and photosynthetic efficiency at low light. The minor changes in pigment ratios we observed within the UML show that mixing rates are higher than rates of

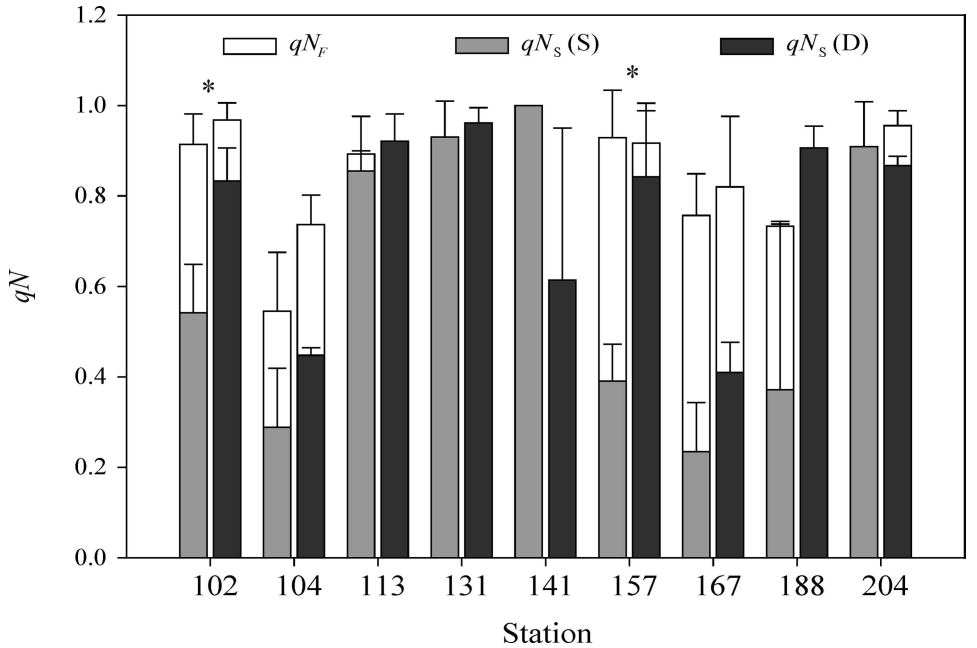

Fig. 6. Results of analysis of fast-relaxing quenching (qN_F) and slow-relaxing quenching (qN_S) of the short-term photoinhibition experiments without the addition of lincomycin. Error bars represent the standard deviation of triplicate analysis. An asterisk represents significant differences in qN_S between surface and subsurface samples (Sta. 102 and 157).

photoacclimation and, therefore, phytoplankton cells acclimate to fluctuating irradiance conditions without having to continuously alter their photophysiology. This is consistent with results from laboratory studies of phytoplankton growing under controlled fluctuating irradiance levels. Generally, the interconversion between dd and dt takes place on short timescales (minutes; Van Leeuwe and Stefels 2007; M. M. Mills unpubl.), whereas ratios of fuc : Chl *a* change over a diel cycle (Van Leeuwe and Stefels 2007). In addition, our data on changes in *Fv* : *Fm* support trends previously observed in studies with Antarctic phytoplankton under fluctuating irradiance regimes, where peaks in irradiance are related to drops in *Fv* : *Fm* (Van Leeuwe et al. 2005; Van Leeuwe and Stefels 2007; Kropuenske et al. 2009) while the *qN* remains stable (A. C. Alderkamp unpubl.) or changes on a timescale of several hours (L. R. Kropuenske unpubl.).

Photosynthetic architecture of oceanic phytoplankton—Significant photoinhibition was observed at all stations investigated when phytoplankton assemblages were exposed to relatively mild surface irradiance conditions, despite differences in species composition between the stations. Species-specific differences in photoprotective strategies have been reported between Antarctic diatoms and Prasinophyceae (Van Leeuwe et al. 2005) and between Antarctic diatoms and *Phaeocystis antarctica* (Kropuenske et al. 2009). Nevertheless, *qN* and photoinhibition characteristics were strikingly similar in all stations investigated in this study. Because all stations were located in open

Table 4. Correlations in simple linear regressions of factor 1, quenching parameters and factor 2, several biological and physical factors in the surface irradiance exposure experiments, considering both surface and subsurface samples. The PAR_{exp} is the average photosynthetically available radiation level during 20 min of surface irradiance exposure in μmol photons m^{-2} s^{-1}, z_{UML} in m, E_{UML} in mol photons m^{-2} d^{-1}, and xanthophyll cycle pigment ratio (dd + dt) : Chl a_{d+h} as described in Table 2.

Sector	Factor 1	Factor 2	Equation	*n*	R^2	*p*
All	qN_S	PAR_{exp}	$qNs=0.0006\times[PAR_{exp}]+0.392$	18	0.280	<0.05
All	qN_F	PAR_{exp}	$qN_F=-0.0004\times[PAR_{exp}]+0.377$	18	0.229	<0.05
All	qN_S	z_{UML}	$qNs=0.0018\times[z_{UML}]+0.579$	18	0.035	0.46
All	qN_F	z_{UML}	$qN_F=-0.0023\times[z_{UML}]+0.330$	18	0.115	0.17
Meridian	qN_F	z_{UML}	$qN_F=-0.0037\times[z_{UML}]+0.455$	14	0.283	0.05
All	qN_S	E_{UML}	$qNs=0.034\times[E_{UML}]+0.584$	18	0.037	0.44
All	qN_F	E_{UML}	$qN_F=-0.019\times[E_{UML}]+0.245$	18	0.023	0.55
All	qN_S	(dd+dt) : Chl a_{d+h}	$qNs=-0.0017\times[(dd+dt) : Chla_{d+h}]+0.692$	18	0.000	0.99
All	qN_F	(dd+dt) : Chl a_{d+h}	$qN_F=-0.134\times[(dd+dt) : Chla_{d+h}]+0.202$	18	0.001	0.89

oceanic regions, off the Antarctic continental shelf, sensitivity to photodamage seems to be a common feature in oceanic phytoplankton.

It is well documented that diatoms and other oceanic phytoplankton have lower Fe requirements than coastal species (Sunda et al. 1991; Sunda and Huntsman 1995). Specifically, oceanic diatoms have evolved a unique photosynthetic architecture to lower their Fe requirements (Strzepek and Harrison 2004), including reduced photosystem I and cytochrome b_6f complex concentrations, both components of the photosystem with high Fe requirements. However, reduced cytochrome b_6f has a negative effect on fast-relaxing non-photochemical quenching (qN_F) (Strzepek and Harrison 2004). The qN_F is mainly regulated by the ΔpH of the thylakoid membrane, produced chiefly through proton translocation by the cytochrome b_6f complex (Price et al. 1995; Munekage et al. 2001; Strzepek and Harrison 2004). Even under Fe-replete conditions, oceanic diatoms showed a lower qN_F than coastal diatoms (Strzepek and Harrison 2004). In concurrence with this, we saw a low qN_F when phytoplankton were exposed for 20 min to surface irradiance at all stations. In addition, the lack of a correlation between (dd + dt) : Chl a_{d+h} and qN_F indicates that proton translocation by the cytochrome b_6f complex may not have been enough to generate the ΔpH of the thylakoid membrane needed for de-epoxidation of the available xanthophyll pigments. The absence of qN_F seems to be a major cause for the significant photoinhibition and photodamage to the D1 reaction center we observed. Although no kinetic analysis of relaxation of quenching was performed when measuring qN in the profiles, this mechanism suggests that slow-relaxing quenching related to photodamage is likely to be a major part of the high qN observed throughout the UML. This notion was confirmed by the observation that prolonging dark acclimation times did not increase the $Fv:Fm$ or qN values (results not shown), unless acclimation times of > 1 h were employed. The low levels of qN_F, its short relaxation time, and the absence of dt in the pigment composition, also suggests that relaxation of qN_F was rapid, in contrast to some studies showing that, in coastal diatoms, de-epoxidation of all dt can take up to 4 h (Kropuenske et al. 2009).

Thus, it is apparent that the photodamage experienced by phytoplankton residing near the ocean surface prevents cells from efficiently using the available light for photosynthesis within the UML. In addition, there are significant costs associated with repair of photodamage. The combination of these two factors likely prevented accumulation of phytoplankton biomass in regions with a deep UML, despite the fact that the levels of E_{UML} were higher than in areas close to the Antarctic continent that had a shallower UML and higher phytoplankton biomass levels.

The importance of D1 repair for maintaining photosynthetic competence—With limited capacity of qN_F in oceanic diatoms to dissipate excess energy during high irradiance exposure, the D1 repair cycle is crucial for maintaining photosynthetic performance for oceanic phytoplankton even under the relatively low irradiance levels they encounter when residing in a deep UML. The same was previously observed during exposure of natural coastal phytoplankton communities from various environments (including the Antarctic) to high levels of ambient solar irradiance (1750–2000 μmol photons m^{-2} s^{-1}; Bouchard et al. 2005*a*,*b*) and in culture studies of an Antarctic coastal diatom *Thalassiosira weissflogii* that was exposed to high irradiance levels (1600 μmol photons m^{-2} s^{-1}; Van de Poll et al. 2007). In this study, blocking D1 repair with lincomycin resulted in cell death after several hours. Thus, an active D1 repair cycle is important for maintaining photosynthetic efficiency for both oceanic and coastal phytoplankton.

These observations of the importance of D1 repair in restoring $Fv:Fm$ during short-term exposure to surface irradiance support the notion that there is a dynamic relationship between photodamage and repair and that the balance between these two processes determines whether phytoplankton become photoinhibited. When the rate of PS II repair balances the rate of photodamage, symptoms of photoinhibition are not apparent in vivo, although the repair process likely imposes increasing metabolic costs. Apparently, rates of D1 repair are consistently too low to keep up with photodamage in the fluctuating light environment of the deep mixed layers of the ACC. There are three likely reasons for this. (1) The low temperatures in the Southern Ocean likely reduce the rate of D1 repair because of both the fundamental temperature effect on enzymatic processes and changes in the thylakoid membrane structure (Greer et al. 1986; Kanervo et al. 1995; reviewed by Bouchard et al. 2006). Indeed, Rae et al. (2000) observed suppression of PS II repair processes by low ambient temperatures in Antarctic microalgae in ponds on the McMurdo ice shelf. (2) Fe limitation reduces D1 synthesis in phytoplankton (Greene et al. 1992), which is also a key step in the PS II repair cycle (reviewed by Bouchard et al. 2006). Therefore, Fe limitation likely reduces D1 repair rates, but to our knowledge no experiments have been performed to test this. In our study, we conducted too few surface irradiance exposure experiments with too many variable factors to see a specific effect of dFe concentrations on repair rates. (3) UVB radiation was found to inhibit D1 repair processes in coastal phytoplankton populations in Antarctica (Bouchard et al. 2005*b*) and other regions (Bouchard et al. 2005*a*). However, UVB radiation could not have influenced D1 repair in our surface irradiance exposure experiments because the phytoplankton were incubated in polystyrene incubation flasks that are transparent to both PAR and UVA, but block UVB. Nevertheless, UVB penetration in the surface waters in the open ocean is known to inhibit D1 repair, thereby enhancing the effects of photodamage in situ.

Phytoplankton growth in HNLC regions—The importance of the z_{UML} for phytoplankton growth in the open ocean has been widely recognized. Shoaling of a deep UML in a given area, as described by Mitchell et al. (1991), leads to a higher E_{UML} that stimulates phytoplankton growth. The effect of the z_{UML} on phytoplankton growth and productivity was also demonstrated in the synthesis of results from seven in situ Fe fertilization experiments. By comparing the response of phytoplankton to Fe additions

Table 5. Correlations of various measures of phytoplankton response to Fe fertilization in seven in situ iron fertilization experiments from De Baar et al. (2005) with z_{UML} and E_{UML}. The max Chl *a* is the maximum observed Chl *a* concentrations during the Fe fertilization experiment in mg m^{-3}. The max ΔNO_3 is the maximum observed removal of nitrate, the max ΔfCO_2 the maximum observed decrease in fugacity of CO_2 in Pa, and the max ΔDIC the maximum observed decrease in dissolved organic carbon in mmol m^{-3}. The z_{UML} is the depth of the upper mixed layer in m. The E_{UML} is the average of the irradiance levels available to phytoplankton in the upper mixed layer in mol photons m^{-2} d^{-1} as published by Boyd et al. (2007) for the seven experiments.

Factor 1	Factor 2	Best fit	*n*	R^2	*p*
Max Chl *a*	z_{UML}	Max Chl $a=523.21\times z_{UML}^{-1.360}$ (exponential)	7	0.90	<0.001
Max ΔNO_3	z_{UML}	Max $\Delta NO_3=82.33\times z_{UML}^{-0.884}$ (exponential)	7	0.69	<0.05
Max ΔfCO_2	z_{UML}	Max $\Delta fCO_2=-0.108\times z_{UML}+9.66$ (linear)	7	0.63	<0.05
Max ΔDIC	z_{UML}	Max $\Delta DIC=-0.772\times z_{UML}+59.04$ (linear)	7	0.72	<0.05
Max Chl *a*	E_{UML}	Max Chl $a=100.27\times E_{UML}^{-1.125}$ (exponential)	7	0.91	<0.001
Max ΔNO_3	E_{UML}	Max $\Delta NO_3=58.01\times E_{UML}^{-0.950}$ (exponential)	7	0.69	<0.05
Max ΔfCO_2	E_{UML}	Max $\Delta fCO_2=-0.220\times E_{UML}+10.06$ (linear)	7	0.62	<0.05
Max ΔDIC	E_{UML}	Max $\Delta DIC=437.82\times E_{UML}^{-0.979}$ (exponential)	7	0.75	<0.05

in environments with a range of physical conditions (temperature, incident irradiance, patch dilution) and biogeochemical responses, De Baar et al. (2005) showed that high biological production is related to a shallow UML in the Southern Ocean, the north Pacific Ocean, and the east equatorial Pacific Ocean (Table 5). This has led to the conclusion that the light climate is an important control on phytoplankton growth in HNLC regions, in addition to the low dFe concentrations. However, as was shown in our research, the z_{UML} does not necessarily vary in the same direction as the E_{UML}, since the latter is also dependent on the attenuation of light within the water column and incident irradiance, which varies with time of year and latitude. Moreover, when the same measures of biological production are correlated with the average levels of E_{UML} of the seven experiments published by Boyd et al. (2007), this correlation appears to be negative (Table 5). Similar to our results on the zero meridian transect, higher measures of biological production in the Fe fertilization experiments correlate with a shallower z_{UML}, but also with lower levels of E_{UML}. This shows that low phytoplankton biomass in regions with a deep UML are not caused by low light levels but rather by photoinhibition during the high-light part of mixing cycle in various HNLC regions, despite vast differences in physical factors such as actual light levels and temperature.

It has been proposed (Strzepek and Harrison 2004; Lavaud et al. 2007) that the fundamental difference between habitats of coastal diatoms that experience large, rapid fluctuations in irradiance (due to turbidity and rapid tidal stirring) and the more stable light climate of the relatively transparent open ocean has decreased the selective pressure on diatoms to retain Fe-costly short-term photoprotective mechanisms, such as the de-epoxidation of dd to dt. Diatoms could, therefore, decrease the amount of Fe needed within photosynthetic electron carriers, which facilitates their continued presence in the open ocean. However, we show that similar to the coastal habitats, rapid mixing in deep wind-mixed upper layers (Cisewski et al. 2005; Croot et al. 2007) of the open ocean can lead to large and rapid fluctuations in irradiance. Our data suggest that the resulting photodamage may be enhanced by the decreased levels of qN_F in oceanic phytoplankton and this poses a serious trade-off to their lower Fe requirements.

Acknowledgments

We thank the captain and crew of R/V *Polarstern* for their support, the cruise leader Eberhard Fahrbach, and all cruise participants for their help and sharing their data. This research was sponsored by the National Science Foundation DynaLiFe program (grant ANT-0732535) in the framework of the United States–International Polar Year program.

References

Allen, J. F. 1995. Thylakoid protein phosphorylation, state 1-state 2 transitions, and photosystem stoichiometry adjustment: Redox control at multiple levels of gene expression. Physiol. Plant. **93:** 196–205, doi:10.1034/j.1399-3054.1995.930128.x

Anderson, J. M., Y.-I. Park, and W. S. Chow. 1997. Photoinactivation and photoprotection of photosystem II in nature. Physiol. Plant. **100:** 214–223, doi:10.1111/j.1399-3054.1997.tb04777.x

Aro, E. M., S. McCaffery, and J. M. Anderson. 1993. Photoinhibition and D1 protein-degradation in peas acclimated to different growth irradiances. Plant Physiol. **103:** 835–843.

Arrigo, K. R., G. L. van Dijken, and M. Long. 2008. Coastal Southern Ocean: A strong anthropogenic CO_2 sink. Geophys. Res. Lett. **35:** L21602, doi:10.1029/2008GL035624

Baker, N. R., and P. Horton. 1987. Physiological factors associated with fluorescence quenching during photoinhibition, p. 145–168. *In* C. J. Arntzen, D. J. Kyle and C. B. Osmond [eds.], Topics in photosynthesis, v. 9: Photoinhibition. Elsevier.

Behrenfeld, M. J., A. J. Bale, Z. S. Kolber, J. Aiken, and P. G. Falkowski. 1996. Confirmation of iron limitation of phytoplankton photosynthesis in the equatorial Pacific Ocean. Nature **383:** 508–511, doi:10.1038/383508a0

Bilger, W., and O. Björkman. 1990. Role of the xanthophyll cycle in photoprotection elucidated by measurements of light-induced absorbency changes, fluorescence and photosynthesis in leaves of Hedera-Canariensis. Photosynth. Res. **25:** 173–185, doi:10.1007/BF00033159

Bouchard, J. N., D. A. Campbell, and S. Roy. 2005a. Effects of UV-B radiation on the D1 protein repair cycle of natural phytoplankton communities from three latitudes (Canada, Brazil, and Argentina). J. Phycol. **41:** 273–286, doi:10.1111/j.1529-8817.2005.04126.x

———, S. Roy, and D. A. Campbell. 2006. UVB effects on the photosystem II-D1 protein of phytoplankton and natural phytoplankton communities. Photochem. Photobiol. **82:** 936–951, doi:10.1562/2005-08-31-IR-666

———, ———, G. Ferreyra, D. A. Campbell, and A. Curtosi. 2005b. Ultraviolet-B effects on photosystem II efficiency of natural phytoplankton communities from Antarctica. Pol. Biol. **28:** 607–618, doi:10.1007/s00300-005-0727-4

Boyd, P. W., and others. 2007. Mesoscale iron enrichment experiments 1993–2005: Synthesis and future directions. Science **315:** 612–617, doi:10.1126/science.1131669

———, and others. 2000. A mesoscale phytoplankton bloom in the polar Southern Ocean stimulated by iron fertilization. Nature **407:** 695–702, doi:10.1038/35037500

Cisewski, B., V. H. Strass, and H. Prandke. 2005. Upper-ocean vertical mixing in the Antarctic Polar Front Zone. Deep-Sea Res. II **52:** 1087–1108, doi:10.1016/j.dsr2.2005.01.010

Croot, P. L., and others. 2007. Physical mixing effects on iron biogeochemical cycling: FeCycle experiment. J. Geophys. Res. **112:** C06015, doi:10.1029/2006JC003748

De Baar, H. J. W., and others. 2005. Synthesis of iron fertilization experiments: From the iron age in the age of enlightenment. J. Geophys. Res. **110:** C09S16, doi:10.1029/2004JC002601

Demmig, B., K. Winter, A. Kruger, and F. C. Czygan. 1987. Photoinhibition and zeaxanthin formation in intact leaves—a possible role of the xanthophyll cycle in the dissipation of excess light energy. Plant Physiol. **84:** 218–224, doi:10.1104/pp.84.2.218

Denman, K. L., and A. E. Gargett. 1983. Time and space scales of vertical mixing and advection of phytoplankton in the upper ocean. Limnol. Oceanogr. **28:** 801–815.

Falkowski, P. G., and J. La Roche. 1991. Acclimation to spectral irradiance in algae. J. Phycol. **27:** 8–14, doi:10.1111/j.0022-3646.1991.00008.x

Geider, R. J., J. La Roche, R. M. Greene, and M. Olaizola. 1993. Response of the photosynthetic apparatus of *Phaeodactylum tricornutum* (Bacillariophyceae) to nitrate, phosphate, or iron starvation. J. Phycol. **29:** 755–766, doi:10.1111/j.0022-3646.1993.00755.x

Greene, R. M., R. J. Geider, Z. Kolber, and P. G. Falkowski. 1992. Iron-induced changes in light harvesting and photochemical energy-conversion processes in eukaryotic marine-algae. Plant Physiol. **100:** 565–575, doi:10.1104/pp.100.2.565

Greer, D. H., J. A. Berry, and O. Björkman. 1986. Photoinhibition of photosynthesis in intact bean-leaves—role of light and temperature, and requirement for chloroplast-protein synthesis during recovery. Planta **168:** 253–260.

Gruber, N., and others. 2009. Oceanic sources, sinks, and transport of atmospheric CO_2. Global Biogeochem. Cycles **23:** GB1005, doi:10.1029/2008GB003349

Hazzard, C., M. P. Lesser, and R. A. Kinzie. 1997. Effects of ultraviolet radiation on photosynthesis in the subtropical marine diatom, *Chaetoceros gracilis* (Bacillariophyceae). J. Phycol. **33:** 960–968, doi:10.1111/j.0022-3646.1997.00960.x

Holm-Hansen, O., A. F. Amos, and C. D. Hewes. 2000. Reliability of estimating chlorophyll *a* concentrations in Antarctic waters by measurement of *in situ* chlorophyll *a* fluorescence. Mar. Ecol. Prog. Ser. **196:** 103–110, doi:10.3354/meps196103

Kanervo, E., E. M. Aro, and N. Murata. 1995. Low unsaturation level of thylakoid membrane-lipids limits turnover of the D1 protein of photosystem-II at high irradiance. FEBS Lett. **364:** 239–242, doi:10.1016/0014-5793(95)00404-W

Kirk, J. T. O. 1994. Light and photosynthesis in aquatic ecosystems. Cambridge Univ. Press.

Kraay, G. W., M. Zapata, and M. J. W. Veldhuis. 1992. Separation of chlorophylls-C1, chlorophylls-C2, and chlorophylls-C3 of marine phytoplankton by reversed-phase-C18 high-performance liquid-chromatography. J. Phycol. **28:** 708–712, doi:10.1111/j.0022-3646.1992.00708.x

Krause, G. H., and E. Weis. 1991. Chlorophyll fluorescence and photosynthesis—the basics. Ann. Rev. Plant Physiol. Plant Mol. Biol. **42:** 313–349, doi:10.1146/annurev.pp.42.060191.001525

Kropuenske, L. R., M. M. Mills, G. L. van Dijken, S. Bailey, D. H. Robinson, N. A. Welschmeyer, and K. R. Arrigo. 2009. Photophysiology in two major Southern Ocean phytoplankton taxa: Photoprotection in *Phaeocystis antarctica* and *Fragilariopsis cylindrus*. Limnol. Oceanogr. **54:** 1176–1196.

Kulheim, C., J. Agren, and S. Jansson. 2002. Rapid regulation of light harvesting and plant fitness in the field. Science **297:** 91–93, doi:10.1126/science.1072359

Lavaud, J., B. Rousseau, H. J. van Gorkom, and A. L. Etienne. 2002. Influence of the diadinoxanthin pool size on photoprotection in the marine planktonic diatom *Phaeodactylum tricornutum*. Plant Physiol. **129:** 1398–1406, doi:10.1104/pp.002014

———, R. F. Strzepek, and P. G. Kroth. 2007. Photoprotection capacity differs among diatoms: Possible consequences on the spatial distribution of diatoms related to fluctuations in the underwater light climate. Limnol. Oceanogr. **52:** 1188–1194.

Mackey, M. D., D. J. Mackey, H. W. Higgins, and S. W. Wright. 1996. CHEMTAX—a program for estimating class abundances from chemical markers: Application to HPLC measurements of phytoplankton. Mar. Ecol. Prog. Ser. **144:** 265–283, doi:10.3354/meps144265

Martin, J. H., R. M. Gordon, and S. E. Fitzwater. 1990. Iron in Antarctic waters. Nature **345:** 156–158, doi:10.1038/345156a0

Mathot, S., J. M. Dandois, and C. Lancelot. 1992. Gross and net primary production in the Scotia-Weddell Sea sector of the Southern Ocean during spring 1988. Pol. Biol. **12:** 321–332, doi:10.1007/BF00238275

Maxwell, K., and G. N. Johnson. 2000. Chlorophyll fluorescence—a practical guide. J. Exp. Bot. **51:** 659–668, doi:10.1093/jexbot/51.345.659

Mitchell, B. G., E. A. Brody, O. Holm-Hansen, C. McClain, and J. Bishop. 1991. Light limitation of phytoplankton biomass and macronutrient utilization in the Southern Ocean. Limnol. Oceanogr. **36:** 1662–1677.

Munekage, Y., S. Takeda, T. Endo, P. Jahns, T. Hashimoto, and T. Shikanai. 2001. Cytochrome b(6)f mutation specifically affects thermal dissipation of absorbed light energy in *Arabidopsis*. Plant J. **28:** 351–359, doi:10.1046/j.1365-313X.2001.01178.x

Neale, P. J., E. W. Helbling, and H. E. Zagarese. 2003. Modulation of UVR exposure and effects by vertical mixing and advection, p. 109–129. *In* E. W. Helbling and H. E. Zagarese [eds.], UV effects in aquatic organisms and ecosystems. Royal Society of Chemistry.

Olaizola, M., J. La Roche, Z. Kolber, and P. G. Falkowski. 1994. Nonphotochemical fluorescence quenching and the diadinoxanthin cycle in a marine diatom. Photosynth. Res. **41:** 357–370, doi:10.1007/BF00019413

Oquist, G., W. S. Chow, and J. M. Anderson. 1992. Photoinhibition of photosynthesis represents a mechanism for the long-term regulation of photosystem-II. Planta **186:** 450–460, doi:10.1007/BF00195327

Price, G. D., J. W. Yu, S. Voncaemmerer, J. R. Evans, W. S. Chow, J. M. Anderson, V. Hurry, and M. R. Badger. 1995. Chloroplast cytochrome b_6f and ATP synthase complexes in tobacco—transformation with antisense RNA against nuclear-encoded transcripts for the Rieske FeS and ATP-δ polypeptides. Austr. J. Plant Physiol. **22:** 285–297, doi:10.1071/PP9950285

Rae, R., C. Howard-Williams, I. Hawes, and W. Vincent. 2000. Temperature dependence of photosynthetic recovery from solar damage in Antarctic phytoplankton, p. 183–189. *In* W. Davison, C. Howard-Williams and P. Broady [eds.], Antarctic ecosystems: Models for wider ecological understanding. Caxton Press.

Riley, G. A. 1957. Phytoplankton of the North Central Sargasso Sea, 1950–52. Limnol. Oceanogr. **2:** 252–270.

Ruban, A. V., and P. Horton. 1995. An investigation of the sustained component of nonphotochemical quenching of chlorophyll fluorescence in isolated chloroplasts and leaves of spinach. Plant Physiol. **108:** 721–726.

Sabine, C. L., and others. 2004. The oceanic sink for anthropogenic CO_2. Science **305:** 367–371, doi:10.1126/science.1097403

Shelly, K., P. Heraud, and J. Beardall. 2003. Interactive effects of PAR and UV-B radiation on PS II electron transport in the marine alga *Dunaliella tertiolecta* (Chlorophyceae). J. Phycol. **39:** 509–512, doi:10.1046/j.1529-8817.2003.02148.x

Strzepek, R. F., and P. J. Harrison. 2004. Photosynthetic architecture differs in coastal and oceanic diatoms. Nature **431:** 689–692, doi:10.1038/nature02954

Sunda, W. G., and S. A. Huntsman. 1995. Iron uptake and growth limitation in oceanic and coastal phytoplankton. Mar. Chem. **50:** 189–206, doi:10.1016/0304-4203(95)00035-P

———, D. G. Swift, and S. A. Huntsman. 1991. Low iron requirement for growth in oceanic phytoplankton. Nature **351:** 55–57, doi:10.1038/351055a0

Van de Poll, W. H., A. C. Alderkamp, P. J. Janknegt, J. Roggeveld, and A. G. J. Buma. 2006. Photoacclimation modulates excessive photosynthetically active and ultraviolet radiation effects in a temperate and an Antarctic marine diatom. Limnol. Oceanogr. **51:** 1239–1248.

———, M. A. van Leeuwe, J. Roggeveld, and A. G. J. Buma. 2005. Nutrient limitation and high irradiance acclimation reduce PAR and UV-induced viability loss in the Antarctic diatom *Chaetoceros brevis* (Bacillariophyceae). J. Phycol. **41:** 840–850, doi:10.1111/j.1529-8817.2005.00105.x

———, R. J. W. Visser, and A. G. J. Buma. 2007. Acclimation to a dynamic irradiance regime changes excessive irradiance sensitivity of *Emiliania huxleyi* and *Thalassiosira weissflogii*. Limnol. Oceanogr. **52:** 1430–1438.

Van Kooten, O., and J. F. H. Snel. 1990. The use of chlorophyll fluorescence nomenclature in plant stress physiology. Photosynth. Res. **25:** 147–150, doi:10.1007/BF00033156

Van Leeuwe, M. A., and J. Stefels. 1998. Effects of iron and light stress on the biochemical composition of Antarctic *Phaeocystis* sp. (Prymnesiophyceae). II. Pigment composition. J. Phycol. **34:** 496–503, doi:10.1046/j.1529-8817.1998.340496.x

———, and ———. 2007. Photosynthetic responses in *Phaeocystis antarctica* towards varying light and iron conditions. Biogeochem. **83:** 61–70, doi:10.1007/s10533-007-9083-5

———, B. van Sikkelerus, W. W. C. Gieskes, and J. Stefels. 2005. Taxon-specific differences in photoacclimation to fluctuating irradiance in an Antarctic diatom and a green flagellate. Mar. Ecol. Prog. Ser. **288:** 9–19, doi:10.3354/meps288009

———, L. A. Villerius, J. Roggeveld, R. J. W. Visser, and J. Stefels. 2006. An optimized method for automated analysis of algal pigments by HPLC. Mar. Chem. **102:** 267–275, doi:10.1016/j.marchem.2006.05.003

Vassiliev, I. R., Z. Kolber, K. D. Wyman, D. Mauzerall, V. K. Shukla, and P. G. Falkowski. 1995. Effects of iron limitation on photosystem-II composition and light utilization in *Dunaliella tertiolecta*. Plant Physiol. **109:** 963–972.

Worby, A., and I. Allison. 1999. A technique for making shipbased observations of Antarctic sea ice thickness and characteristics. Part I: Observational technique and results. Research Report 14. Antarctic CRC.

Wright, S. W., A. Ishikawa, H. J. Marchant, A. T. Davidson, R. L. van den Enden, and G. V. Nash. 2009. Composition and significance of picophytoplankton in Antarctic waters. Pol. Biol. **32:** 797–808, doi:10.1007/s00300-009-0582-9

———, D. P. Thomas, H. J. Marchant, H. W. Higgins, M. D. Mackey, and D. J. Mackey. 1996. Analysis of phytoplankton of the Australian sector of the Southern Ocean: Comparisons of microscopy and size frequency data with interpretations of pigment HPLC data using the 'CHEMTAX' matrix factorisation program. Mar. Ecol. Prog. Ser. **144:** 285–298, doi:10.3354/meps144285

Zapata, M., S. W. Jeffrey, S. W. Wright, F. Rodriguez, J. L. Garrido, and L. Clementson. 2004. Photosynthetic pigments in 37 species (65 strains) of Haptophyta: Implications for oceanography and chemotaxonomy. Mar. Ecol. Prog. Ser. **270:** 83–102, doi:10.3354/meps270083

Associate editor: Heidi M. Sosik

Received: 14 August 2009
Accepted: 10 January 2010
Amended: 09 February 2010